# The PI3Kδ-Selective Inhibitor Idelalisib Minimally Interferes With Immune Effector Function Mediated by Rituximab or Obinutuzumab and Significantly Augments B Cell Depletion In Vivo

**Running title:** MINIMAL INTERFERENCE OF IDELALISIB WITH IMMUNE EFFECTOR FUNCTION

Adam Palazzo,* Sylvia Herter,† Laura Grosmaire,* Randy Jones,* Christian Frey,* Marina Bacac,† Pablo Umana,† Robert J. Oldham,‡ Michael J. E. Marshall,‡ Kerry L. Cox,‡ Anna H. Turaj,‡ Mark S. Cragg,‡ Christian Klein,† Matthew J. Carter,‡,# and Stacey L. Tannheimer*,#

*Gilead Sciences, Inc., Foster City, California, USA; †Roche Pharmaceutical Research and Early Development, Roche Innovation Center Zurich, Switzerland; and ‡Antibody and Vaccine Group, Cancer Sciences Unit, Faculty of Medicine, University of Southampton, Southampton, United Kingdom

# M.J.C. and S.L.T. are joint senior authors.

A.P., C.F., M.S.C., and C.K. designed the research plan; A.P., S.H., L.G., R.J., M.B., P.U., M.J.C., R.O., M.M., K.C., and A.T. conducted research; A.P., S.H., L.G., M.S.C., and C.K. performed data analysis; and A.P., M.J.C., M.S.C., C.K., and S.L.T. did manuscript drafting and review.

**Address correspondence and reprint requests to** Adam Palazzo, Gilead Sciences, Inc., 199 East Blaine Street, Seattle, Washington, USA. Email address: adam.palazzo@gilead.com [phone 206-454-7109, fax 206-832-1965]

21 Keywords: CD20, Natural Killer Cells, Cytotoxicity, Phagocytosis, Idelalisib

22

**Abstract**

Idelalisib is a highly selective oral inhibitor of phosphoinositide 3-kinase-delta (PI3Kδ) indicated for the treatment of patients with relapsed chronic lymphocytic leukemia in combination with rituximab. Despite additive clinical effects, previous studies have paradoxically demonstrated that targeted therapies potentially negatively affect anti-CD20 mAb effector mechanisms. To address these potential effects, we investigated the impact of PI3Kδ inhibition by idelalisib on the effector mechanisms of rituximab and obinutuzumab. At clinically relevant concentrations, idelalisib minimally influenced rituximab- and obinutuzumab-mediated Ab-dependent cellular cytotoxicity and phagocytosis on human lymphoma cell lines, while maintaining the superiority of obinutuzumab-mediated Ab-dependent cellular cytotoxicity. Consistent with this, idelalisib did not influence obinutuzumab-mediated B cell depletion in whole blood B cell depletion assays. Further, idelalisib significantly enhanced obinutuzumab-mediated direct cell death of chronic lymphocytic leukemia cells. In murine systems, in vivo inhibition of PI3Kδ minimally interfered with maximal rituximab- or obinutuzumab-mediated depletion of leukemic targets. In addition, the duration of both rituximab- and obinutuzumab-mediated depletion of leukemia cells was extended by combination with PI3Kδ inhibition. Collectively, these data demonstrate that PI3Kδ inhibition does not significantly affect the effector mechanisms of rituximab or obinutuzumab and provides an effective therapeutic combination in vivo. Therefore, combinations of obinutuzumab and idelalisib are currently being assessed in clinical studies,.

## Introduction

PI3Kδ represents the most prominent PI3K isoform in B lymphocytes. As such, PI3Kδ is central to multiple signaling pathways that drive the proliferation, survival, homing, and retention of malignant B cells within primary and secondary lymphoid organs. Accordingly, PI3Kδ represents a prime target for therapeutic intervention in B cell malignancies and is effectively targeted by idelalisib, a highly selective oral inhibitor of PI3Kδ (1, 2). Idelalisib functions by selective prevention of ATP binding to the catalytic domain of PI3Kδ, thereby preventing phosphorylation of phosphatidylinositol and subsequent serine/threonine protein kinase B phosphorylation (3). In the United States, idelalisib is indicated, in combination with rituximab, for the treatment of patients with relapsed chronic lymphocytic leukemia (CLL) and as monotherapy for relapsed follicular B cell non-Hodgkin lymphoma (FL) and relapsed small lymphocytic lymphoma (4). In the European Union, idelalisib is indicated, in combination with rituximab or ofatumumab, for the treatment of patients with relapsed CLL, as first-line therapy in CLL patients with the 17p deletion or *TP53* mutation who are deemed unsuitable for chemoimmunotherapy, and as monotherapy for patients with refractory FL (5).

Type I anti-CD20 mAbs, such as rituximab, rapidly induce the redistribution of CD20 within the plasma membrane to a low-density, detergent-insoluble membrane compartment, which may affect binding properties and effector functions that control the therapeutic effect of anti-CD20 mAbs (6, 7). In contrast, type II anti-CD20 mAbs (such as obinutuzumab) do not induce significant CD20 redistribution and as such impart enhanced therapeutic effects, including direct killing of cellular targets by homotypic adhesion (7–9). In addition to its type II properties, obinutuzumab is glycoengineered and consequently offers enhanced affinity for FcγRIII and

increased ADCC and Ab-dependent cellular phagocytosis (ADCP) in comparison to rituximab (10, 11).

Obinutuzumab has been approved for the first-line treatment of CLL patients in combination with chlorambucil in the United States and Europe and for first line treatment of fNHL in Europe based on head-to-head trials comparing obinutuzumab containing regimen to the respective rituximab containing regimen using a flat dose of 1000 mg for obinutuzumab and 375 mg/m2 for rituximab, as well as for the treatment of rituximab-refractory FL patients (12, 13). In first-line diffuse large B cell lymphoma obinutuzumab did not show no superior outcome (15).

Because anti-CD20 mAbs are standard of care, it is important to understand whether new targeted agents affect their function. Previous work has shown that the covalent Bruton's tyrosine kinase (BTK) inhibitor ibrutinib can interfere with immune effector function and, ultimately, in vivo efficacy of rituximab in preclinical models (16). Because PI3K isoforms also play a role in immune effector cells and FcγR signaling (17), we investigated the effect of PI3Kδ inhibition by idelalisib on the immune effector functions of rituximab and obinutuzumab and the efficacy of in vivo anti-CD20 mAb therapy in a murine model of CLL.

## Materials and Methods

*Reagents and chemicals*

Idelalisib was synthesized at Gilead Sciences, Inc. (Foster City, CA), dissolved in DMSO at 10 mM and stored at –20°C. Rituximab and obinutuzumab were provided by Hoffmann-La Roche AG (Basel, Switzerland). Palivizumab was used as a negative control and was produced at Gilead Sciences, Inc.

*Cell culture*

WIL2-S cells were obtained from the American Type Culture Collection (Manassas, VA) and maintained in IMDM, supplemented with 10% ultra-low Ig FBS and 1% penicillin-streptomycin (all Life Technologies [Thermo Fisher Scientific], Grand Island, NY). Z-138 cells were a gift from Dr. Martin Dyer at the University of Leicester and maintained in RPMI 1640 with 10% FCS and 1% GlutaMAX (Thermo Fisher Scientific). Frozen CLL PBMC target cells were thawed and washed in RPMI with 10% FCS (Sigma Aldrich, St. Louis, MO), 2 mM glutamine, 1 mM sodium pyruvate, 100 U/ml penicillin, and 100 μg/ml streptomycin (all Life Technologies) before resuspending in PBS (Severn Biotech Ltd., Kidderminster, UK) at $1 \times 10^7$ cells/ml. Effector cells (PBMCs) were isolated from anonymized leukocyte cones (University of Southhampton Tissue Bank, Southampton, UK) using lymphoprep (AXIS-SHIELD, Alere Technologies AS, Oslo, Norway) density gradient centrifugation. The buffy coat layer was removed with a pasteur pipette, washed three times with PBS (2 mM EDTA) at 300 × *g* and resuspended in RPMI at $20 \times 10^6$ cells/ml. NK cells were enriched from leukapheresis blood product derived from healthy donors (AllCells, Alameda, CA). PBMCs were isolated by standard Ficoll density gradient centrifugation technique, and NK cells were enriched using a

negative-selection immunomagnetic enrichment kit (Stem Cell Technologies, Vancouver, Canada) according to the manufacturer's instructions. Enriched NK cells were incubated overnight in RPMI 1640 with GlutaMAX supplemented with 10% ultra-low Ig FBS and 1% penicillin-streptomycin at 37°C in a 5% $CO_2$ incubator before NK cells were used for experiments.

For macrophage polarization, frozen $CD14^+$ monocytes enriched by negative selection were thawed and cultured in T75 tissue flasks in AIM-V media (Life Technologies) with 60 ng/ml M-CSF (PeproTech, Rocky Hill, NJ). On day 7, monocyte-derived macrophages (MDMs) were washed and plated in AIM-V with polarizing cytokines. For differentiation to M1 macrophages, cells were plated for 24 h in 100 ng/ml IFN-γ (R&D Systems, Minneapolis, MN), and 100 ng/ml LPS (derived from *E. coli* strain 055:B5, Sigma Aldrich), and for M2c macrophages, cells were plated for 48 h in 10 ng/ml IL-10 (R&D Systems).

*ADCC assay*

PBMCs were prepared by Histopaque (Sigma Aldrich) density centrifugation of fresh blood obtained from healthy human donors. WIL2S target cells ($2.5 \times 10^4$ cells/well) were incubated with human isolated PBMCs ($6.25 \times 10^5$ cells/well), as well as titrations of obinutuzumab or rituximab (0.01–1000 ng/ml) in the presence or absence of 256 nM idelalisib in AIM-V medium for 4 h in a humidified incubator at 37°C,5% $CO_2$. 10 µl/well of a 1:10 pre-dilution of anti-CD107a-PE Ab (BioLegend 328608 [San Diego, CA]) was added into the culture to determine NK cell degranulation. Tumor cell lysis was assessed after 4 h of incubation at 37°C, 5% $CO_2$ by quantification of lactate dehydrogenase (LDH) released into cell culture supernatants (LDH detection kit, Roche Applied Science, #11 644 793 001). Maximal lysis of the target cells

(=100%) was achieved by incubation of target cells with 2% Triton X-100. Spontaneous release (=0%) refers to target cells coincubated with effector cells without Abs. ADCC was calculated using the following formula:

$$\text{Percentage ADCC} = \left( \left[ \frac{\text{sample release} - \text{spontaneous release}}{\text{maximal release} - \text{spontaneous release}} \right] \right) \times 100.$$

For the assessment of NK cell degranulation, surface staining for CD3 (PE-Cy7, anti-human CD3 Ab, BioLegend, 300420) and CD56 (APC anti-human CD56, BioLegend, 318310) was performed. After 30 min incubation at 4°C in the dark, cells were washed twice with 150 µl/well PBS/0.1% BSA and fixed using 100 µl/well BD FACS Lysing Solution (BD Biosciences, 349202). Samples were analyzed using a BD FACSCanto II.

WIL2-S were resuspended at $2 \times 10^6$ cells/ml in ADCC assay media consisting of RPMI without phenol red (Life Technologies) supplemented with 1% low Ig FBS (Life Technologies) and 1% penicillin-streptomycin. Target cells were plated in a 96-well, deep-well plates in triplicate. Idelalisib or 0.2% DMSO was added to target cells and incubated for 40 min at 37°C in 5% $CO_2$. Obinutuzmab, rituximab, or palivizumab were prepared in ADCC assay media. After incubation for 40 min in compound or vehicle, each Ab was added to target cells and incubated at room temperature for 20 min before ADCC assay setup. Effector cells (PBMCs or enriched NK cells) were incubated with idelalisib or 0.2% DMSO and incubated for 1 h at 37°C, 5% $CO_2$. Effector cells were added to wells containing target cells to reach an E:T ratio in a range from 1:1–30:1 comparable to those used by Kohrt et al (16). Control wells included target cells alone with mAbs in combination with and without idelalisib, as well as target cells alone. Additionally, effector cells alone in the presence or absence of idelalisib were plated as controls. The plates were incubated for 4 h at 37°C in a 5% $CO_2$ incubator. LDH release was measured using a

cytotoxicity detection kit (Roche Applied Science, Indianapolis, IN) following the manufacturer's instructions. Absorbance values were measured using a SpectraMax microplate reader (Molecular Devices, Sunnyvale, CA) set at 490 nM with a reference wavelength at 650 nM. ADCC was calculated using the previously described formula. Percent of maximum was calculated using the following formula: $100 - ([(\text{normal activity} - \text{inhibited activity}) \div (\text{normal activity})] \times 100)$ with normal activity being the percent of ADCC without the addition of idelalisib.

CLL Cells: Frozen CLL PBMC target cells were thawed and washed in media before resuspending in PBS (Severn Biotech) at $1 \times 10^7$ cells/ml. Ten microliters of calcein AM (1 mg/ml, Life Technologies) was added per milliliter, and cells were incubated at 37°C in 5% $CO_2$ for 30 min with periodic mixing. Cells were washed three times (300 × *g*, 5 min) with PBS (10% FCS) and resuspended in media at $9 \times 10^5$ cells/ml. Effector cells (PBMCs) were isolated from anonymized leukocyte cones (University of Southhampton Tissue Bank, Southampton, UK) using lymphoprep (AXIS-SHIELD) density gradient centrifugation and resuspended in media at $20 \times 10^6$ cells/ml. Target and effector cells were separately preincubated with either no drug, vehicle (DMSO), or idelalisib (1 μM to 1 nM) for 40 min at 37°C in 5% $CO_2$. A total of 90 μl of target cells were transferred to a round-bottomed, 96-well plate (Thermo Fisher Scientific), and Ab was added to a final concentration of 10 μg/ml. Cells were incubated for an additional 20 min, after which 100 μl of effector cells with matching pretreatment were added (E:T ratio, 25:1) and the plate briefly pulse centrifuged and incubated for 4 h at 37°C, 5% $CO_2$. After incubation, the plate was centrifuged at 200 × *g* for 5 min and 90 μl of supernatant transferred to a white-walled, 96-well plate. Calcein release was measured using a VarioSkan plate reader (Thermo Fisher Scientific; excitation 494 nM, emission 515 nM) and lysis calculated as a percentage of

maximum lysis (4% Triton X-100) after subtraction of background (target cells plus effector cells without Ab).

*ADCP assay*

Idelalisib was added to plated macrophages in AIM-V media and incubated at 37°C for 1 h, followed by addition of rituximab or obinutuzumab. WIL2-S target cells were labeled with CellTracker Red (CTR; Molecular Probes; Thermo Fisher Scientific) as per the manufacturer's protocol and then combined with the macrophages at an E:T ratio of 3:1. The cocultures were incubated for 2 h at 37°C. Cells were then stained with FITC anti-CD14 (BD Biosciences) and FITC anti-CD11b (eBioSciences) and analyzed on an LSR II cytometer (BD Biosciences).

Cells within the live cell gate containing $CD14^+$ M1 or M2c macrophages and $CTR^+$ target cells were further separated within a dot plot quadrant. $FITC^+$ effector macrophages were placed in the upper left quadrant of the *y*-axis and $CTR^+$ target cells in the lower right quadrant of the *x*-axis. Double positive cells ($FITC^+CTR^+$) in the upper right quadrant represent phagocytized target cells, and percent phagocytosis was calculated as

$$(\%\ \text{double positive cell} \div [\%\ \text{double postive cells} + \%\ \text{target cells alone}]) \times 100.$$

*B cell depletion in human whole blood*

Normal B cell depletion was also assessed using fresh heparinized human blood from healthy volunteers. Briefly, fresh blood was collected in heparin-containing syringes. Blood aliquots (180 µl/well) were placed into 96-well, deep-well plates, supplemented with 10 µg/ml obinutuzumab or rituximab (10 µl/well) in the absence or presence of idelalisib and incubated for 1 day at 37°C in 5% $CO_2$ in a humidified cell incubator. After incubation, blood was mixed by

pipetting up and down before 35 µl/well blood aliquots were transferred in 96-well, round-bottom plates and incubated with fluorescent anti-CD45 (anti-human CD45 APC, BioLegend, 304037), anti-CD19 (anti-human CD19 PE, BioLegend, 302208), and anti-CD3 (anti-human CD3 PECy7, BioLegend, 300420). After 15 min incubation at room temperature, FACS lysis solution (BD Biosciences) was added to lyse erythrocytes and to fix cells prior to flow cytometry. B cell depletion was evaluated using Ab-untreated samples as a 100% control and the following formula:

$$100 - \left( \left[ \frac{100}{\text{B/T cell ratio in control}} \right] \right) \times \left( \left[ \text{B/T cell ratio in sample containing antibody} \right] \right).$$

The average B cell depletion and standard deviations of the triplicates of each experiment were calculated.

*CLL cell death assay*

CLL subject whole blood was obtained through Bioreclamation (Westbury, NY), and PBMCs were collected by Ficoll separation and cryopreserved in freezing medium (50% IMDM, 40% FBS, and 10% DMSO). Frozen primary CLL PBMCs were thawed, washed, and rested for 3–5 h in RPMI 1640, 10 mM HEPES, pH 7.4, 1 mM sodium pyruvate, 2 mM GlutaMAX, 55 µM ß-mercaptoethanol, 100 U/ml penicillin/streptomycin, 10% FBS at 37°C prior to plating. Cells were then plated at 1.0–2.5 × $10^6$ cells/ml in combination with idelalisib and antibodies. Assay plates were incubated for 1 h prior to stimulation with αIgM/αIgG (20 µg/ml) and αCD40 (20 µg/ml). Cells were incubated at 37°C with 5% $CO_2$ for 66 h. Cells were transferred to a deep-well plate and washed with 1 ml cation-free PBS ($PBS^{-/-}$). Cells were resuspended in Live/Dead Aqua (Life Technologies) according to manufacturer's instructions. After viability staining, cells

were labeled with CD5-PE, CD19-BV421, and annexin V-APC, washed, fixed with 4% paraformaldehyde, and acquired on a CantoII cytometer (BD Biosciences). $CD5^+CD19^+$ cells were identified and gated for analysis. The $CD5^+CD19^+$ population was plotted annexin V-APC vs live/dead. Quadrant gates were drawn where Q1 is annexin $V^-$ and live/$dead^+$, Q2 is annexin $V^+$ and live/$dead^+$, Q3 is annexin $V^+$ and live/$dead^-$, and Q4 is double negative. Results are reported as the sum of Q1, Q2, and Q3 as a percent of the total cells.

*Animals*

Mice were maintained in local facilities and experiments approved by local ethical committees under UK Home Office license PPL# PB24EEE31. Eμ-TCL1 transgenic (Tg) mice were obtained from Dr. Egle (Salzburg Cancer Research Institute, Salzburg, Austria) with the consent of Dr. Pekarsky and Professor Croce (Ohio State University, Ohio, USA). Eμ-TCL1 Tg animals were crossed with human CD20 Tg C57BL/6 mice (a kind gift from Professor Shlomchik, University of Pittsburgh School of Medicine, Pittsburgh, USA), previously described in Ahuja et al (18) and monitored for disease presentation. Terminal animals were sacrificed and splenocytes harvested and cryopreserved. Sex-matched C57BL/6 or severe combined immunodeficiency syndrome (SCID) mice were inoculated with $1 \times 10^7$ splenocytes derived from Eμ-TCL1 Tg or CD20 Tg Eμ-TCL1 Tg mice, respectively, and monitored for disease presentation by weekly blood sampling and flow cytometry. Following disease presentation, mice were treated with 250 μg anti-mouse CD20 (clone 18B12 mouse IgG2a), 250 μg rituximab (hIgG1), or 250 μg obinutuzumab (hIgG1) by i.p. injection alongside 10 mg/kg GS-9820 per os BID or an appropriate vehicle control, as described previously (19). Disease progression/therapeutic responses were subsequently monitored by blood sampling and flow cytometry.

## Results

*Impact of idelalisib on immune effector functions of rituximab and obinutuzumab*

The potential impact of idelalisib on the immune effector functions of rituximab and obinutuzumab was first evaluated by measuring ADCC against B cell lymphoma line WIL2S in primary PBMC cultures with titrated amounts of Ab, in the presence or absence of a single concentration of idelalisib, representative of the cell culture medium protein-binding–adjusted maximum peak concentration ($C_{max}$) of 256 nM. As expected, the magnitude of ADCC mediated by obinutuzumab was greater than that of rituximab, and the addition of idelalisib showed little to no effect on ADCC with either Ab (Fig. 1A). Effector NK cell surface expression analysis by flow cytometry showed a concentration-dependent increase in the frequency of $CD107a^+$ NK cells with both rituximab and obinutuzumab, with obinutuzumab inducing more profound effects than rituximab (Fig. 1B). Addition of idelalisib reduced the frequency of $CD107a^+$ cells and density of surface CD107a (data not shown) with both obinutuzumab and rituximab starting at 0.1 ng/ml and 10 ng/ml, respectively. When ADCC was evaluated over varying E:T ratios using isolated NK cells (effectors) and WIL2-S (target) and at saturating concentrations of rituximab and obinutuzumab (10 µg/ml), idelalisib had no effect on ADCC when tested over a dose range from 5–500 nM (Fig. 2).

The effect of idelalisib over a range of concentrations (1-1000 nM) was evaluated in ADCC assays using a fixed E:T ratio and saturating amounts of obinutuzumab or rituximab. Idelalisib did not affect rituximab- or obinutuzumab-mediated ADCC in the context of the maximal ADCC activity of each anti-CD20 Ab (Fig. 3A). The impact of FcγRIIIa genotype was assessed with NK effectors derived from donors with FcγRIIIa 158 phenylalanine homozygous (F/F),

phenylalanine/valine (F/V), or valine homozygous (V/V) genotypes. Idelalisib at concentrations up to 1 μM had no significant effect on rituximab- or obinutuzumab-mediated ADCC in FcγRIIIa 158 F/F and F/V genotypes (Fig. 3B). ADCC with the FcγRIIIa 158V/V effectors was slightly affected by treatment with idelalisib (~15% inhibition) at the highest concentration tested.

*Impact of idelalisib on ADCC with primary CLL specimens*

Next, obinutuzumab- or rituximab-mediated ADCC in the presence of idelalisib using primary CLL PBMCs as targets was assessed. Both obinutuzumab and rituximab were effective at inducing ADCC at a saturating concentration of Ab (10 μg/ml), with obinutuzumab inducing 47% ADCC and rituximab inducing 20% ADCC (Fig. 3C-D). The amount of ADCC remained largely unchanged for both Abs in combination with idelalisib over a clinically relevant concentration range.

In addition to ADCC, the effects of idelalisib on obinutuzumab- and rituximab-mediated ADCP were assessed. Primary human MDMs were generated, polarized, and ADCP with obinutuzumab or rituximab evaluated. ADCP with both Abs was more robust with M2c-directed macrophages (rituximab 61 ± 8%, obinutuzumab 57 ± 14%) than M1 (rituximab 20 ± 5%, obinutuzumab 20 ± 2%). M2c- and M1-polarized macrophages maintained their ability to effectively phagocytose target cells at up to 300 nM idelalisib, equal to the protein-adjusted $C_{max}$ (Fig. 4A, 4B).

*Whole blood Ab-mediated B cell depletion in the presence of idelalisib*

The effects of idelalisib in an autologous B cell depletion assay using a dose-titration of obinutuzumab was assessed in the presence of clinically relevant concentrations of idelalisib

(760 nM and 4200 nM, minimal concentration [$C_{min}$] and [$C_{max}$]in whole blood). In both donors, B cells were depleted dose dependently in the presence of increasing concentrations of obinutuzumab (Fig. 5A). Although there was a slight trend toward inhibition of B cell depletion in one donor, there were no statistically significant effects with idelalisib across the range of obinutuzumab concentrations. Autologous B cell depletion was also tested in the presence of titrated idelalisib (54–6810 nM) in combination with saturating concentrations of either obinutuzumab or rituximab in three donors. B cell depletion by obinutuzumab was largely unaffected by idelalisib (Fig. 5B). In contrast, B cell depletion by rituximab in combination with idelalisib varied across donors, with the most inhibition seen only at the highest concentration. In all donors tested, idelalisib alone showed no B cell depletion at any concentrations.

*Direct induction of cell death in primary CLL specimens*

Next, we examined the ability of idelalisib, obinutuzumab, or the combination to induce direct cell death in primary CLL cultures, stimulated with anti-IgM/IgG/CD40 to mimic prosurvival signaling within the tissues. Idelalisib (30–480 nM) showed a small but significant increase in cell death (8–10%) across all doses, whereas obinutuzumab (0.5–5 μg/ml) showed a dose-dependent induction of cell death of 2–21%, most prominent at 5 μg/ml (Fig. 6). However, more striking was the ability of the combination of idelalisib (480 nM) and obinutuzumab (5 μg/ml) to elicit a statistically significant increase in cell death (39%) above either single agent alone.

*In vivo therapy of Eμ-TCL1 Tg leukemia-bearing mice*

We next assessed the impact of PI3Kδ inhibition upon the extent and duration of anti-CD20–mediated B cell depletion in a murine model of CLL, the Eμ-TCL1 Tg mouse model (20). Owing to the unsuitability of idelalisib for use in a murine setting due to unfavorable pharmacokinetic

properties (19; Gilead Sciences, Inc., unpublished observations), we utilized the structurally related surrogate PI3Kδ inhibitor GS-9820. Treatment of leukemia-bearing animals with a suboptimal dose (250 μg/mouse) of anti-mouse CD20 (18B12 mouse IgG2a), or anti-human CD20 mAb (rituximab or obinutuzumab [250 μg/mouse both $hIgG_1$ ]) imparted a rapid and significant reduction in the leukemic burden of treated animals 48 h post-treatment (Fig. 7A). Consistent with previous studies, initial depletion of target cells with obinutuzumab outperformed that achieved with rituximab ($p<0.005$). In this model system, concomitant PI3Kδ inhibition (via GS-9820) induced a statistically significant reduction in the extent of obinutuzumab-mediated depletion and a trend toward reduction in both rituximab and 18B12 treatment settings. In a monotherapy setting, GS-9820 provided a modest therapeutic benefit and effectively reduced the extent of leukemia deposits within secondary lymphoid organs (19) (Fig. 7B, 7C and supplementary figure). Therefore, the apparent reduction in anti-CD20–mediated depletion 48 h post-treatment in the presence of PI3Kδ inhibition may reflect a redistribution of target cells into the periphery, as is observed in clinical trials (21), rather than inhibition of Ab effector mechanisms. In support of this, concomitant administration of a PI3Kδ inhibitor to a single dose of either anti-mouse or anti-human CD20 mAbs provided a more durable depletion of leukemic cells over the long term and significantly enhanced overall survival in comparison to Ab therapy alone (Fig. 7B, 7C). Although obinutuzumab appeared to outperform rituximab in a short-term depletion setting, significant variation in the long-term superiority of one agent over the other was observed between Eμ-TCL1 Tg tumour lines (supplementary figure). This observation is most likely attributable to the suboptimal nature of the antibody dosing strategy. These data identify that, despite the marginal impact of PI3Kδ inhibition on in vitro Ab effector

mechanism assays and in vivo depletion in the first 48 h with obinutuzumab, these combinations provide additional benefit in the duration of leukemic depletion in a therapeutic model.

## Discussion

The recent regulatory approvals of multiple new targeted therapies, including the anti-CD20 mAb obinutuzumab, have provided many treatment options for patients with CLL. Multiple small molecule inhibitors that target the BCR pathway have been approved for use in CLL, with idelalisib approved for use with rituximab in relapsed and refractory CLL (4, 5). A key step in the clinical integration of these therapies is a clear understanding of how these agents might be combined. Our studies evaluated the effect of idelalisib (or its surrogate GS-9820) at physiologically relevant concentrations on direct killing, ADCC, ADCP, and in vivo therapy in combination with rituximab or obinutuzumab. Rituximab is a type I Ab, whereas obinutuzumab is a type II glycoengineered Ab that has enhanced affinity for FcγRIIIa on effector cells, which leads to enhanced ADCC (11, 22). Differences between the two classes of Abs have also been shown for direct cell killing (9, 23), complement-dependent cytotoxicity (6), and binding-induced CD20 internalization (24), but they seem to have comparable effects on ADCP (10, 25, 26).

Our results using both obinutuzumab and rituximab in ADCC assays corroborate previous studies that show obinutuzumab is better at ADCC regardless of the CD20 levels of the target, Ab concentration, or E:T ratio used in the assay (10). Our studies showed that idelalisib had no effect on anti-CD20 ADCC with either obinutuzumab or rituximab, in contrast to other studies that utilized higher concentrations than are used in the clinic (27, 28). Previous reports have shown that the F/V polymorphism of FcγRIIIa can impact both NK cell binding to Ab (29), as well as progression-free survival when evaluated in the context of rituximab treatment in genotyped patients (30).

When the impact of idelalisib was assessed in vitro on NK cells with known FcγRIIIa polymorphisms, idelalisib showed no inhibition of ADCC regardless of genotype. Our findings also demonstrated that F/F and F/V polymorphisms were no less effective in ADCC cell assays with obinutuzumab. Characterization of NK cells from PI3Kδ kinase-dead or knockout mice show altered NK cell migration, extravasation, receptor activation, and cytokine production, although alterations in cytotoxicity toward tumor cells in vitro or in vivo was not observed (31–33). In our in vitro studies investigating the effects of idelalisib on NK cell-mediated ADCC, not only did we see a lack of inhibition of NK cell function, but we also observed that CD20 levels on the target cells are not altered by PI3Kδ inhibition (data not shown). Additionally, unlike ibrutinib, which has been shown to suppress ADCC and ADCP function due to strong inhibition of IL-2–inducible tyrosine kinase (ITK), idelalisib has no activity on BTK or ITK (16, 34, 35).

MDMs, polarized to either M2c or M1, showed robust phagocytosis of target cells, with M2c demonstrating superior activity. Idelalisib had no effect on macrophage ADCP function on either subset up to the protein-adjusted $C_{max}$ concentration of ~300 nM. The robust phagocytosis of myeloid cells in this in vitro assay suggests that idelalisib treatment has little to no impact on macrophage function. More significantly, there is no effect of idelalisib on anti-CD20–mediated B cell depletion from whole blood in healthy donors, an assay that may best model the clinical experience due to the integration of multiple mechanisms for depletion (i.e., ADCC, complement-dependent cytotoxicity, induction of cell death). In agreement with these findings, the coadministration of a surrogate PI3Kδ inhibitor (GS-9820) alongside suboptimal doses of anti-mouse CD20, rituximab, or obinutuzumab only minimally influenced maximal depletion of leukemic targets in a murine model of CLL in vivo. These observations indicate that key Ab effector mechanisms are not significantly affected in vivo by PI3Kδ inhibition and any apparent

368 reduction in anti-CD20–mediated depletion in the presence of PI3Kδ inhibition may reflect a
369 redistribution of target cells into the periphery, as is observed in clinical trials (21). More
370 significantly in this model, coadministration of PI3Kδ inhibition alongside anti-CD20 mAbs
371 imparted a more durable depletion of leukemic targets and enhanced therapeutic effects. These
372 observations are reminiscent of clinical trial results demonstrating the therapeutic enhancement
373 of rituximab therapy offered by coadministration of idelalisib in relapsed CLL patients (21).

374 When the combination of idelalisib with obinutuzumab was evaluated in terms of cell death
375 induction of primary donor CLL cells, strong additive anti-tumor activity was confirmed. This
376 unexpected enhanced activity, in conjunction with the lack of idelalisib inhibition of
377 obinutuzumab-mediated ADCC and ADCP activity, suggests that a glycoengineered type II anti-
378 CD20 Ab may function as effectively as, or better than, a type I Ab in combination with
379 idelalisib.

380 In conclusion, at clinically relevant doses, idelalisib does not have significant effects on
381 rituximab- or obinutuzumab-driven ADCC, ADCP, or B cell depletion activity. Additionally, the
382 obinutuzumab and idelalisib combination appears to have additive activities on direct killing of
383 CLL cells and control of leukemic burden in vivo as compared with either agent alone. These
384 studies provide preclinical rationale that the addition of idelalisib to type II antibodies such as
385 obinutuzumab are likely to be effective clinically without negatively impacting any Ab-mediated
386 immune functions. Based on these findings obinutuzumab is being/has been tested in
387 combination with idelalisib in clinical trials (NCT02962401, NCT02968563, NCT01980875,
388 NCT02445131).

389

**Acknowledgments**

We thank Beth Sesler, PhD, CMPP, of Impact Communication Partners, Inc., for the editorial support. We are grateful to the University of Southampton, Faculty of Medicine Human Tissue Bank (Human Tissue Authority license 12009) and to I. Tracy, I. Henderson, and K. N. Potter for the assistance with collecting and characterizing clinical material.

## References


1. Lannutti, B. J., S. A. Meadows, S. E. M. Herman, A. Kashishian, B. Steiner, A. J. Johnson, J. C. Byrd, J. W. Tyner, M. M. Loriaux, M. Deininger, B. J. Druker, K. D. Puri, R. G. Ulrich, and N. A. Giese. 2011. CAL-101, a p110δ selective phosphatidylinositol-3-kinase inhibitor for the treatment of B-cell malignancies, inhibits PI3K signaling and cellular viability. *Blood.* 117: 591–594.

2. Puri, K. D., and M. R. Gold. 2012. Selective inhibitors of phosphoinositide 3-kinase delta: modulators of B-cell function with potential for treating autoimmune inflammatory diseases and B-cell malignancies. *Front Immunol.* 3: 256. doi:10.3389/fimmu.2012.00256. eCollection 2012.

3. Vanhaesebroeck, B., J. Guillermet-Guibert, M. Graupera, and B. Bilanges. 2010. The emerging mechanisms of isoform-specific PI3K signalling. *Nat Rev Mol Cell Biol.* 11: 329–341.

4. ZYDELIG [package insert]. Foster City, CA: Gilead Sciences, Inc.; 2016.

5. Zydelig [summary of product characteristics]. Cambridge, UK: Gilead Sciences International Ltd.; 2014.

6. Cragg, M. S., S. M. Morgan, H. T. Chan, B. P. Morgan, A. V. Filatov, P. W. M. Johnson, R. R. French, and M. J. Glennie. 2003. Complement-mediated lysis by anti-CD20 mAb correlates with segregation into lipid rafts. *Blood*. 101: 1045–1052.

7. Cragg, M. S., and M. J. Glennie. 2004. Antibody specificity controls in vivo effector mechanisms of anti-CD20 reagents. *Blood.* 103: 2738–2743.

8. Deans, J. P., S. M. Robbins, M. J. Polyak, and J. A. Savage. 1998. Rapid redistribution of CD20 to a low density detergent-insoluble membrane compartment. *J Biol Chem*. 273: 344–348.

9. Ivanov, A., S. A. Beers, C. A. Walshe, J. Honeychurch, W. Alduaij, K. L. Cox, K. N. Potter, S. Murray, C. H. T. Chan, T. Klymenko, J. Erenpreisa, M. J. Glennie, T. M. Illidge, and M. S. Cragg. 2009. Monoclonal antibodies directed to CD20 and HLA-DR can elicit homotypic adhesion followed by lysosome-mediated cell death in human lymphoma and leukemia cells. *J Clin Invest.* 119: 2143–2159.

10. Herter, S., F. Herting, O. Mundigl, I. Waldhauer, T. Weinzierl, T. Fauti, G. Muth, D. Ziegler-Landesberger, E. Van Puijenbroek, S. Lang, M. N. Duong, L. Reslan, C. A. Gerdes, T. Friess, U. Baer, H. Burtscher, M. Weidner, C. Dumontet, P. Umana, G. Niederfellner, M. Bacac, and C. Klein. 2013. Preclinical activity of the type II CD20 antibody GA101 (obinutuzumab) compared with rituximab and ofatumumab *in vitro* and in xenograft models. *Mol Cancer Ther.* 12: 2031–2042.

11. Mössner, E., P. Brünker, S. Moser, U. Püntener, C. Schmidt, S. Herter, R. Grau, C. Gerdes, A. Nopora, E. van Puijenbroek, C. Ferrara, P. Sondermann, C. Jäger, P. Strein, G. Fertig, T. Friess, C. Schüll, S. Bauer, J. Dal Porto, C. Del Nagro, K. Dabbagh, M. J. S. Dyer, S. Poppema, C. Klein, and P. Umaña. 2010. Increasing the efficacy of CD20 antibody therapy through the engineering of a new type II anti-CD20 antibody with enhanced direct and immune effector cell-mediated B-cell cytotoxicity. *Blood.* 115: 4393–4402.

12. GAZYVA [package insert]. South San Francisco, CA: Genentech, Inc.; 2016.

13. Gazyvaro [summary of product characteristics]. Welwyn Garden City, UK: Roche Registration Ltd.; 2014.

14. Marcus, R. E., A. J. Davies, K. Ando, W. Klapper, S. Opat, C. J. Owen, E. H. Phillips, R. Sangha, R. Schlag, J. F. Seymour, W. Townsend, M. Trněný, M. K. Wenger, G. Fingerle-Rowson, K. Rufibach, T. Moore, M. Herold, and W. Hiddemann. Obinutuzumab-based induction and maintenance prolongs progression-free survival in patients with previously untreated follicular lymphoma: primary results of the randomized phase 3 GALLIUM study. Abstract presented at: ASH 58th Annual Meeting & Exposition. December 3-6, 2016; San Diego, CA. Abstract 6. https://ash.confex.com/ash/2016/webprogram/Paper94744.html. Accessed January 20, 2017.

15. Vitolo, U., M. Trněný, D. Belada, A. M. Carella, N. Chua, P. Abrisqueta, J. Demeter, I. W. Flinn, X. Hong, W. S. Kin, A. Pinto, J. M. Burke, Y. Shi, Y. Tatsumi, M. Oestergaard, M. K. Wenger, G. Fingerle-Rowson, O. Catalani, T. Nielsen, M. Martelli, and L. H. Shen. Obinutuzumab or rituximab plus CHOP in patients with previously untreated diffuse large B-cell lymphoma: final results from an open-label, randomized phase 3 study (GOYA). Abstract presented at: ASH 58th Annual Meeting & Exposition. December 3-6, 2016; San Diego, CA. Abstract 470. https://ash.confex.com/ash/2016/webprogram/Paper96159.html. Accessed January 20, 2017.

16. Kohrt, H. E., I. Sagiv-Barfi, S. Rafiq, S. E. Herman, J. P. Butchar, C. Cheney, X. Zhang, J. J. Buggy, N. Muthusamy, R. Levy, A. J. Johnson, and J. C. Byrd. 2014. Ibrutinib antagonizes rituximab-dependent NK cell–mediated cytotoxicity. *Blood.* 123: 1957–1960.

17. Okkenhaug, K. 2013. Signalling by the phosphoinositide 3-kinase family in immune cells. *Annu Rev Immunol.* 31: 675–704.

18. Ahuja, A., J. Shupe, R. Dunn, M. Kashgarian, M. R. Kehry, and M. J. Shlomchik. 2007. Depletion of B cells in murine lupus: efficacy of resistance. *J Immunol.* 179: 3351–3361.

19. Carter, M. J., K. L. Cox, S. J. Blakemore, A. H. Turaj, R. J. Oldham, L. N. Dahal, S. Tannheimer, F. Forconi, G. Packman, and M. S. Cragg. 2016. PI3Kδ inhibition elicits anti-leukemic effects through Bim-dependent apoptosis. *Leukemia.* doi:10.1038/leu.2016.333.

20. Bichi, R., S. A. Shinton, E. S. Martin, A. Koval, G. A. Calin, R. Cesari, G. Russo, R. R. Hardy, and C. M. Croce. 2002. Human chronic lymphocytic leukemia modeled in mouse by targeted TCL1 expression. *Proc Natl Acad Sci U S A.* 99: 6955–6960.

21. Furman, R. R., J. P. Sharman, S. E. Coutre, B. D. Cheson, J. M. Pagel, P. Hillmen, J. C. Barrientos, A. D. Zelenetz, T. J. Kipps, I. Flinn, P. Ghia, H. Eradat, T. Ervin, N. Lamanna, B. Coiffier, A. R. Pettitt, S. Ma, S. Stilgenbauer, P. Cramer, M. Aiello, D. M. Johnson, L. L. Miller, D. Li, T. M. Jahn, R. D. Dansey, M. Hallek, and S. M. O'Brien. 2014. Idelalisib and rituximab in relapsed chronic lymphocytic leukemia. *N Engl J Med*. 370: 997–1007.

22. Ferrara, C., S. Grau, C. Jäger, P. Sondermann, P. Brünker, I. Waldhauer, M. Hennig, A. Ruf, A. C. Rufer, M. Stihle, P. Umaña, and J. Benz. 2011. Unique carbohydrate–carbohydrate interactions are required for high affinity binding between FcγRIII and antibodies lacking core fucose. *Proc Natl Acad Sci U S A*. 108: 12669–12674.

23. Chan, H. T., D. Hughes, R. R. French, A. L Tutt, C. A. Walshe, J. L. Teeling, M. J. Glennie, and M. S. Cragg. 2003. CD20-induced lymphoma cell death is independent of both caspases and its redistribution into triton X-100 insoluble membrane rafts. *Cancer Res*. 63: 5480–5489.

24. Beers, S. A., R. R. French, H. T. C. Chan, S. H. Lim, T. C. Jarrett, R. M. Vidal, S. S. Wijayaweera, S. V. Dixon, H. Kim, K. L. Cox, J. P. Kerr, D. A. Johnston, P. W. M. Johnson, J. Sjef Verbeek, M. J. Glennie, and M. C. Cragg. 2010. Antigenic modulation limits the

efficacy of anti-CD20 antibodies: implications for antibody selection. *Blood.* 115: 5191–5201.

25. Bologna L., E. Gotti, M. Manganini, A. Rambaldi, T. Intermesoli, M. Introna. J. Golay. 2011. Mechanism of action of type II, glycoengineered, anti-CD20 monoclonal antibody GA101 in B-chronic lymphocytic leukemia whole blood assays in comparison with rituximab and alemtuzumab. *J Immunol*. 186: 3762-3769.

26. Rafiq S., J.P. Butchar, C. Cheney, X. Mo, R. Trotta, M. Caligiuri, D. Jarjoura, S. Tridandapani, N. Muthusamy and J. C. Byrd. 2013. Comparative Assessment of Clinically Utilized CD20-Directed Antibodies in Chronic Lymphocytic Leukemia Cells Reveals Divergent NK Cell, Monocyte, and Macrophage Properties. *J Immunol*. 190: 2702-2711.

27. Da Roit, F., P. J. Engelberts, R. P. Taylor, E. C. W. Breji, G. Gritti, A. Rambaldi, M. Introna, P. W. H. I. Parren, F. J. Beurskens, and J. Golay. 2015. Ibrutinib interferes with the cell-mediated anti-tumor activities of therapeutic CD20 antibodies: implications for combination therapy. *Haematologica.* 100: 77–86.

28. Duong, M. N., E-L. Matera, D. Mathé, A. Evesque, S. Valsesia-Wittman, B. Clémenceau, and C. Dumontet. 2015. Effect of kinase inhibitors on the therapeutic properties of monoclonal antibodies. *MAbs*. 7: 192–198.

29. Koene, H. R., M. Kleijer, J. Algra, D. Roos, A. E. G. Kr. von dem Borne, and M. de Haas. 1997. FcγRIIIa-158V/F polymorphism influences the binding of IgG by natural killer cell FcγRIIIa, independently of the FcγRIIIa-48L/R/H phenotype. *Blood.* 90: 1109–1114.

505 30. Cartron, G., L. Dacheux, G. Salles, P. Solal-Celigny, P. Bardos, P. Colombat, and H. Watier.
506 2002. Therapeutic activity of humanized anti-CD20 monoclonal antibody and polymorphism
507 in IgG Fc receptor FcγRIIIa gene. *Blood.* 99: 754–758.

508 31. Guo, H., A. Samarakoon, B. Vanhaesebroeck, and S. Malarkannan. 2008. The p110δ of PI3K
509 plays a critical role in NK cell terminal maturation and cytokine/chemokine generation. *J Exp*
510 *Med.* 205: 2419–2435.

511 32. Saudemont, A., F. Garçon, H. Yadi, M. Roche-Molina, N. Kim, A. Segonds-Pinchon, A.
512 Martin-Fontecha, K. Okkenhaug, and F. Colucci. 2009. p110γ and p110δ isoforms of
513 phosphoinositide 3-kinase differentially regulate natural killer cell migration in health and
514 disease. *Proc Natl Acad Sci U S A.* 106: 5795–5800.
515 33. Kim, N., A. Saudemont, L. Webb, M. Camps, T. Ruckle, E. Hirsch, M. Turner, and F.
516 Colucci. 2007. The p110delta catalytic isoform of PI3K is a key player in NK-cell
517 development and cytokine secretion. *Blood.* 110: 3202–3208.

518 34. Khurana, D., L. N. Arneson, R. A. Schoon, C. J. Dick, and P. J. Leibson. 2007. Differential
519 regulation of human NK cell-mediated cytotoxicity by the tyrosine kinase Itk. *J Immunol.*
520 178: 3575–3582.
521 35. Somoza, J. R., D. Koditek, A. G. Villaseñor, N. Novikov, M. H. Wong, A. Liclican, W.
522 Xing, L. Lagpacan, R. Wang, B. E. Schultz, G. A. Papalia, D. Samuel, L. Lad, and M.. E.
523 McGrath ME. 2015. Structural, biochemical, and biophysical characterization of idelalisib
524 binding to phosphoinositide 3-kinase δ. *J Biol Chem.* 290: 8439–8446.

**Footnotes:** This work and editorial support for manuscript development were funded by Gilead Sciences, Inc. The Tissue Bank was partly funded through Cancer Research UK (C34999/A18087) and Experimental Cancer Medicine Centre grants (C24563/A15581).

**Disclosures:** A.P., L.G., R.J., C.F., and S.L.T. are employees of Gilead Sciences, Inc. and also own stock/shares in Gilead Sciences, Inc. S.H., M.B., P.U., and C.K. are employees of Roche. M.M. is a BBSRC iCASE student with M.S.C. and C.K. M.S.C. acts as a consultant for Bioinvent International and has previously received research grant support from Roche and Gilead Sciences, Inc. M.J.C. is the recipient of a career track fellowship from the University of Southampton and has received travel and accommodation support from Gilead Sciences, Inc.

**Abbreviations:** ADCC, Ab-dependent cellular cytotoxicity; ADCP, Ab-dependent cellular phagocytosis; CLL, chronic lymphocytic leukemia; $C_{max}$, maximum peak concentration; CTR, CellTracker Red; E:T ratio, effector to target ratio; F/F, phenylalanine homozygous; FL, follicular lymphoma; F/V, phenylalanine/valine; LDH, lactate dehydrogenase; mAb, monoclonal antibody; MDMs, monocyte-derived macrophages; PI3Kδ, phosphoinositide 3-kinase-delta; Tg, transgenic; V/V, valine homozygous.

**FIGURE 1**. Effect of idelalisib on anti-CD20–mediated ADCC using healthy donor PBMC. (**A**) Human PBMCs were used as effectors with the –WIL2S cell line at an E:T ratio of 25:1. Anti-CD20 mAb potency was assessed by LDH release after 4 h in the presence or absence of idelalisib (256 nM) over a range of Ab concentrations (0.01–1000 ng/ml) (*n* = 3, in triplicate). (**B**) PBMCs were analyzed from the ADCC assay for %CD107a$^{+}$ cells by gating on CD3$^{-}$ CD56$^{intermediate}$ population (NK cells) and median fluorescence determined for CD107a by flow cytometry as a measure of NK cell degranulation.

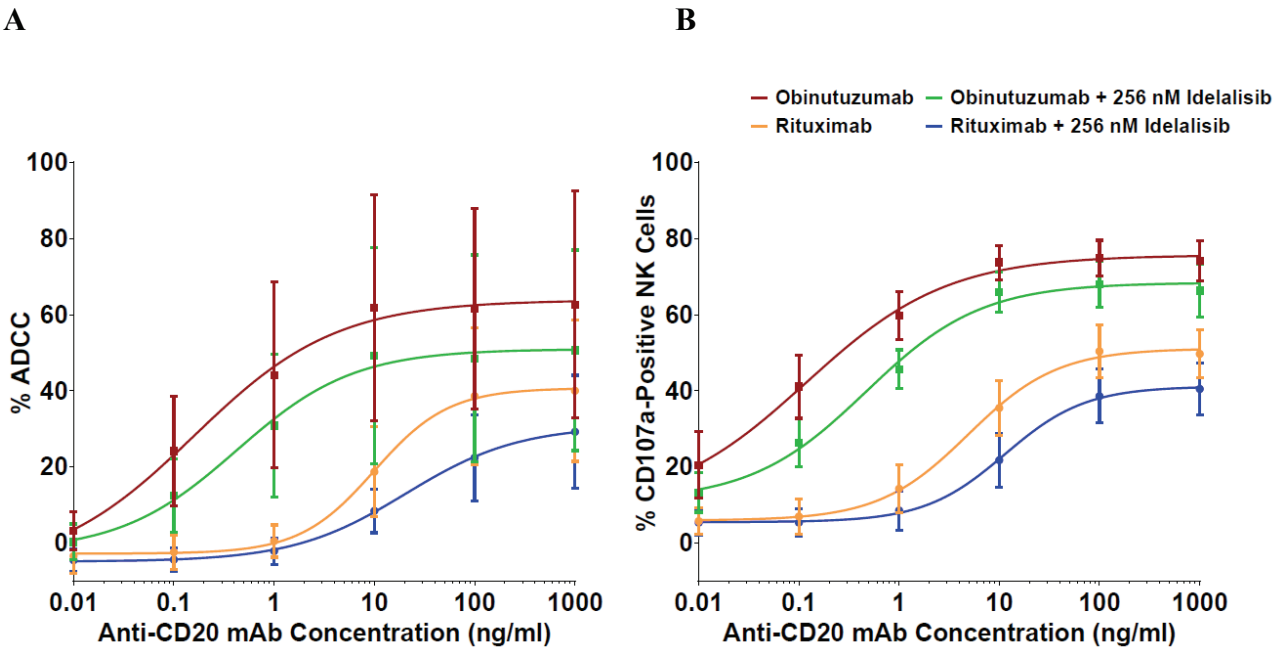

**FIGURE 2.** Idelalisib did not have an effect on ADCC mediated by (**A**) rituximab or (**B**) obinituzumab with healthy donor NK cells. Enriched NK cells were used as effectors with the WIL2-S cell line as target over varying E:T ratios. Anti-CD20 mAb potency was assessed at a saturating concentration (10 µg/ml) in the presence or absence of idelalisib (5–500 nM) by LDH release after 4 h ($n$ = 3, in triplicate). Palivizumab was used as a negative control Ab. NK cells and WIL2-S were incubated without Ab as an Ab-independent cellular cytotoxicity (AICC) control.

**A**

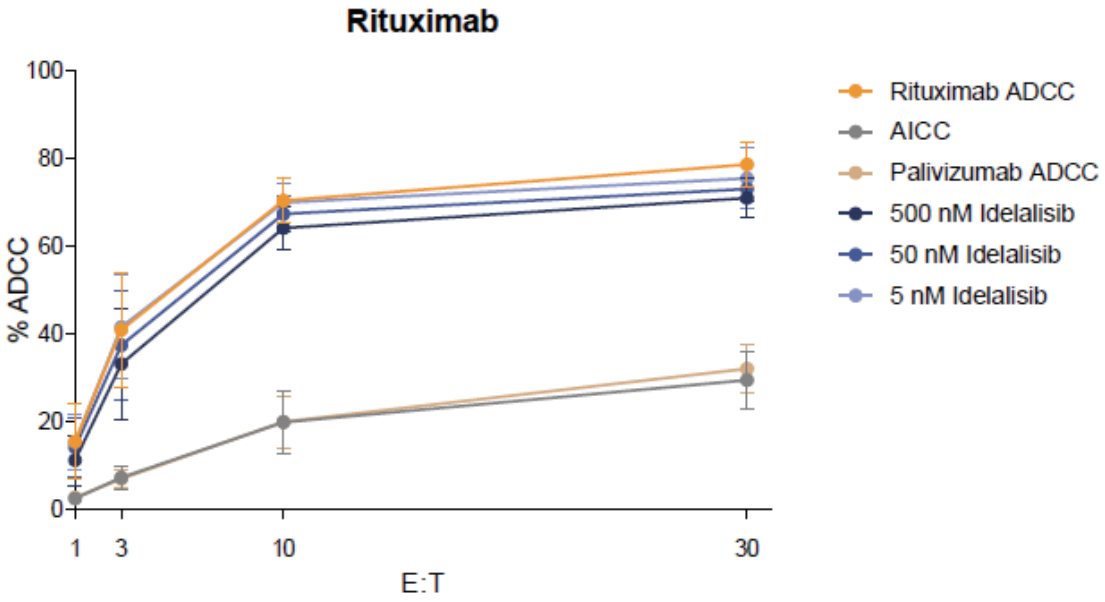

**B**

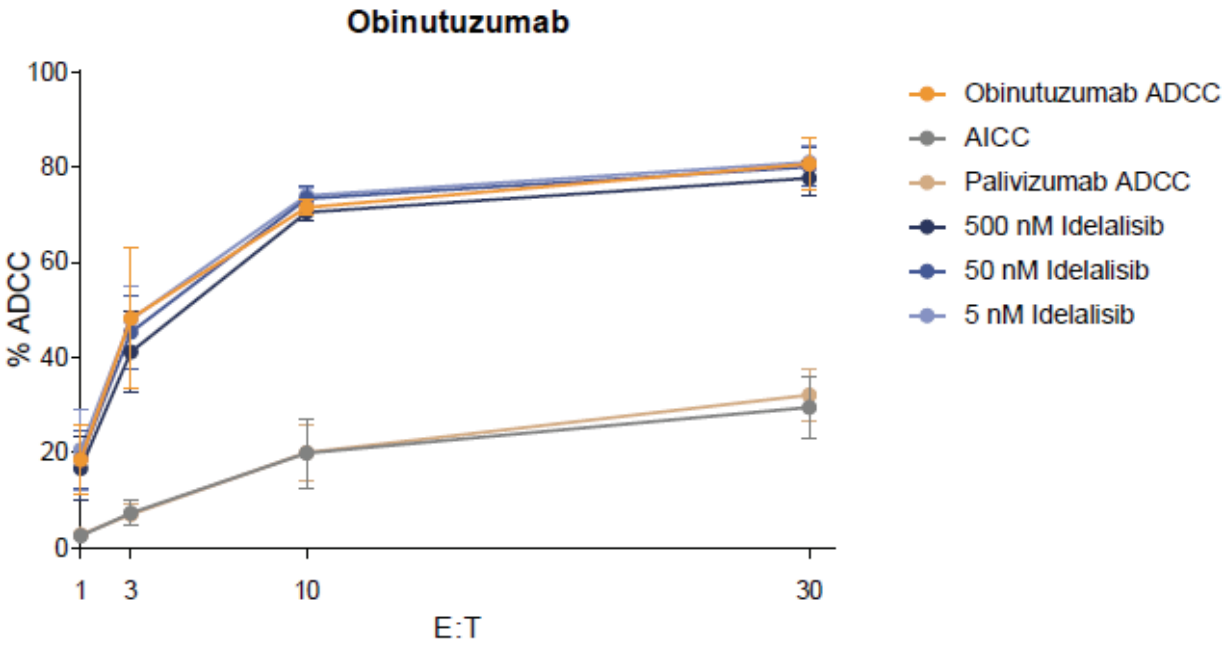
Obinutuzumab
100
80
60
40
20
0
% ADCC
1
3
10
30
E:T
Obinutuzumab ADCC
AICC
Palivizumab ADCC
500 nM Idelalisib
50 nM Idelalisib
5 nM Idelalisib

547

**FIGURE 3**. Effect of idelalisib on anti-CD20–mediated ADCC: impact of effectors, targets, and FcγRIIIa genotype. (**A**) Enriched NK cells were used as effectors with the WIL2-S cell line (E:T ratio, 10:1) and saturating anti-CD20 mAb (10 μg/ml), with the maximum ADCC measured by LDH release after 4 h. Idelalisib activity was assessed (1-1000nM) in combination with anti-CD20 mAb and normalized to percent of maximum cytotoxicity for each donor with Ab only (*n* = 9, in triplicate). (**B**) The role of FcγRIIIa polymorphisms was assessed in enriched NK cells of the 158 F/F, F/V, and V/V genotypes (*n* = 2 of each) in an ADCC as described above. (**C and D**) Human PBMCs were used as effectors with CLL cells as targets at an E:T ratio of 25:1. Anti-CD20 mAb potency was assessed by calcein release after 4 h in the presence of a range of concentrations of idelalisib (1–1000 nM) and a single Ab concentration (10 μg/ml) using obinutuzumab (**C**) or rituximab (**D**) (*n* = 4).

**A**

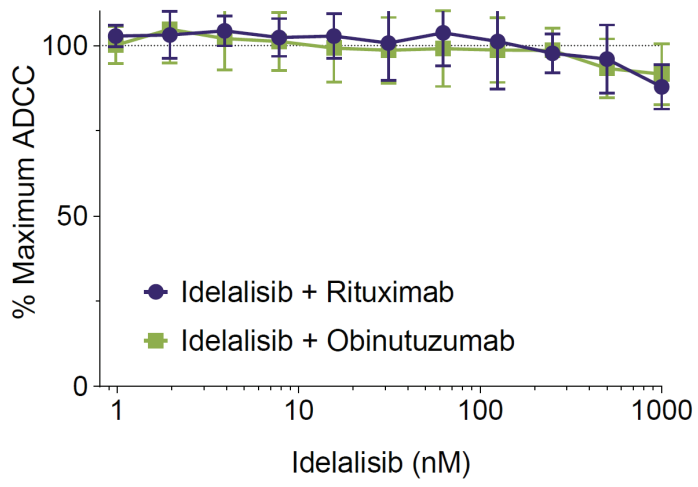

**B**

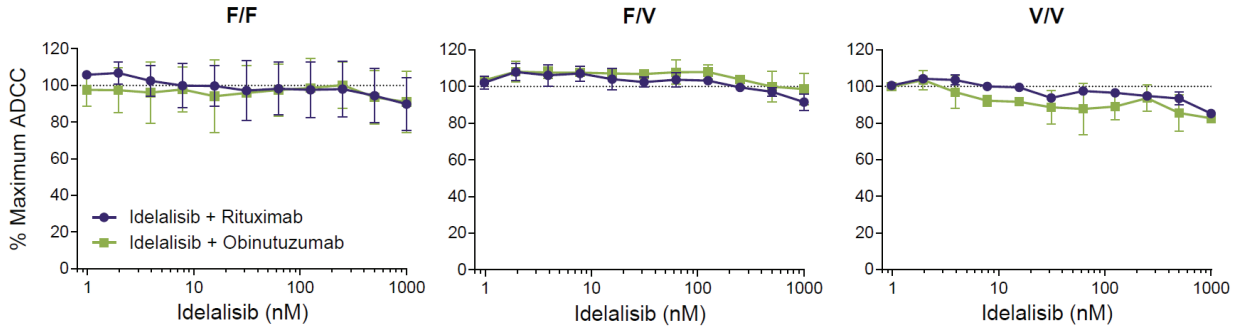
F/F
F/V
V/V
% Maximum ADCC
Idelalisib + Rituximab
Idelalisib + Obinutuzumab
Idelalisib (nM)

**C**

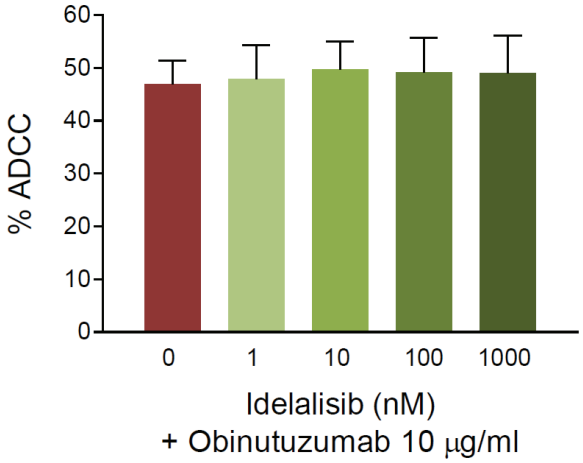
% ADCC
Idelalisib (nM)
+ Obinutuzumab 10 μg/ml

**D**

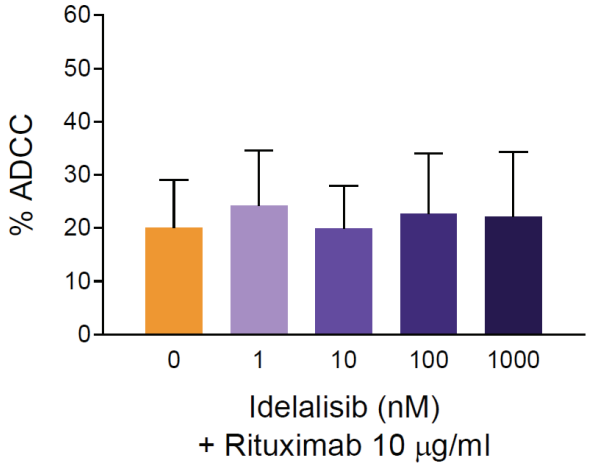
% ADCC
Idelalisib (nM)
+ Rituximab 10 μg/ml

**FIGURE 4**. Effect of idelalisib on anti-CD20–mediated ADCP with M2c- and M1-polarized macrophages. MDMs were polarized in vitro toward M2c-phenotype (**A**) or M1-phenotype (**B**) and used in ADCP assays with WIL2-S cell line as targets (E:T ratio, 3:1) to evaluate the activity of idelalisib (3-1000nM) in the presence of anti-CD20 mAb (150 ng/ml). Percent phagocytosed target cells were quantified by flow cytometry and normalized to ADCP activity with Ab alone (*n* = 3, in triplicate).

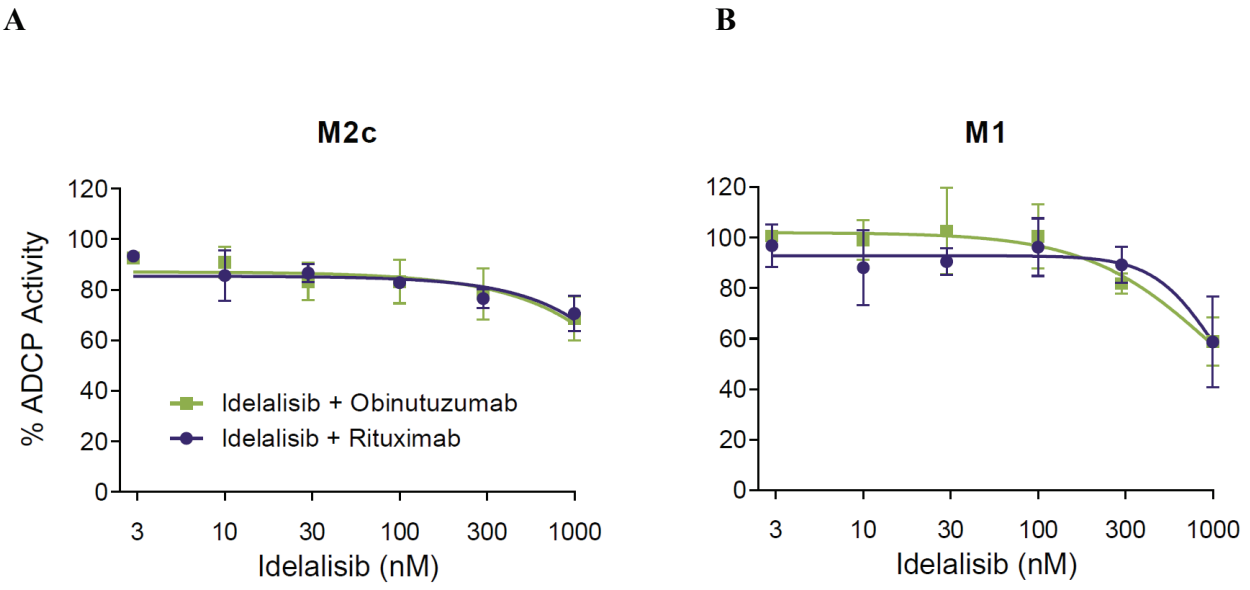

**FIGURE 5**. Effect of idelalisib on anti-CD20–mediated whole blood B cell depletion from healthy volunteers. (**A**) Dose-dependent B cell depletion with obinutuzumab in the presence of clinically relevant concentrations of idelalisib (760 nM and 4200 nM, $C_{min}$ and $C_{max}$ in whole blood) in two representative donors. (**B**) B cell depletion in the presence of a dose-titration of idelalisib (54-6810 nM) in combination with saturating concentrations of either obinutuzumab or rituximab (10 µg/ml; the dotted line represents Ab alone effect) in three representative donors. $CD45^+$ cells were gated, and the depletion of B cells ($CD19^+$) was calculated by flow cytometry.

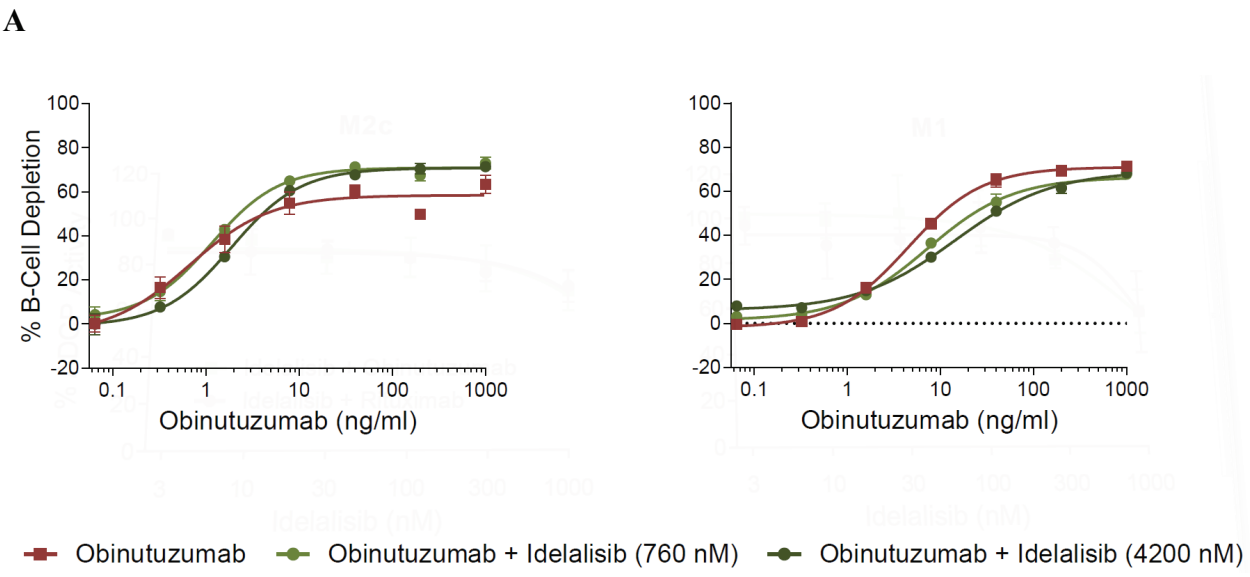


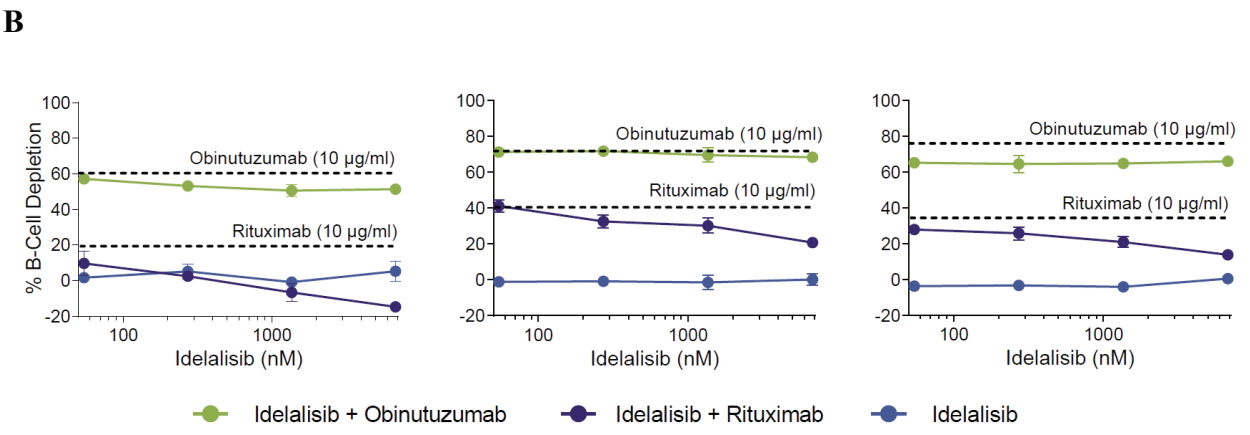

**FIGURE 6.** Effect of idelalisib and obinutuzumab on direct cell death induction of CLL cells. Increasing concentrations of idelalisib (30–480 nM) or obinutuzumab (0.5–5 μg/ml), or a combination of 480 nM idelalisib plus 5 μg/ml obinutuzumab, were added to CLL cultures stimulated with anti-IgM/IgG/CD40 and incubated for 66 h. CLL cells were gated as $CD5^+/CD19^+$ double positive and annexin $V^+$/viable cells and quantitated by flow cytometry ($n$ = 12, in triplicate). Statistical comparisons are pairwise comparisons in the same donor.

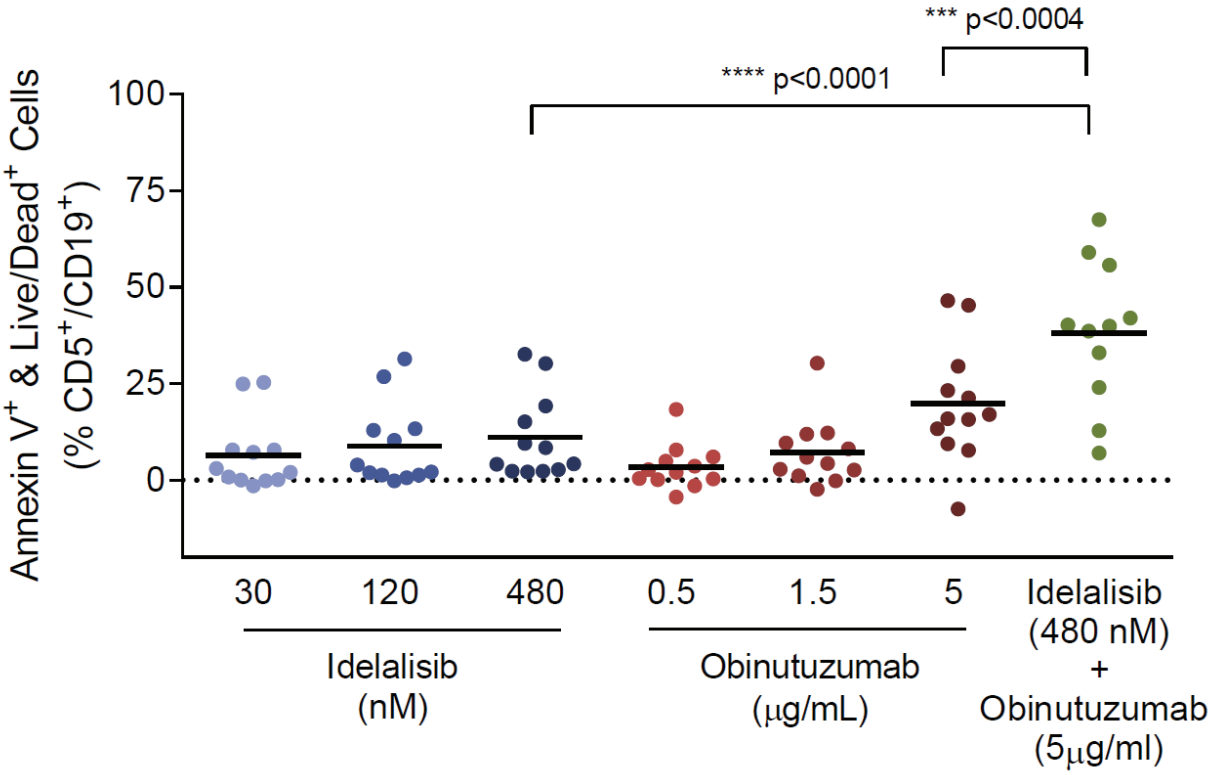

**FIGURE 7**. Anti-CD20–mediated depletion of leukemic targets in vivo. (**A**) Animals bearing either Eμ-TCL1 Tg (left) or human CD20 Tg Eμ-TCL1 Tg leukemias (right) were treated with 250 μg anti-CD20 mAbs (anti-mouse CD20 clone 18B12 mIgG2a, rituximab hIgG1 (RTX), obinutuzumab hIgG1 (OBZ)) alongside 10 mg/kg GS-9820 administered per o.s. BID or an appropriate vehicle control and monitored for peripheral leukemia levels 48 hours later by flow cytometry. Data are normalized to pre-treatment values. (**B**) Eμ-TCL1 Tg tumor (Eμ-TCL1 Tg 020) bearing animals from (A) were maintained on PI3Kδ inhibition treatment or an appropriate vehicle control for the duration of the experiment and monitored for leukemia levels by weekly blood sampling and flow cytometry. The middle panel demonstrates a representative example of the peripheral leukemic fraction 4 weeks post-treatment, expressed as % of total lymphocytes. GS denotes GS9820. (**C**) Human CD20 Tg Eμ-TCL1 Tg tumor (hCD20 Tg Eμ-TCL1 Tg FU2) bearing animals from (A) were maintained on PI3Kδ inhibition treatment or an appropriate vehicle control for the duration of the experiment and monitored for leukemia levels by weekly blood sampling and flow cytometry. Data are represented as %$CD5^+$ $B220^+$ present in the lymphocyte gate. Statistical analyses were performed by paired/unpaired Student *t*-test in (A) and two-way ANOVA or log-rank survival analysis in (B–C). *$p < 0.05$, **$p < 0.005$, ***$p <$

595 0.0005, ****$p < 0.000005$. ns, not statistically significant. Error bars represent SEM.

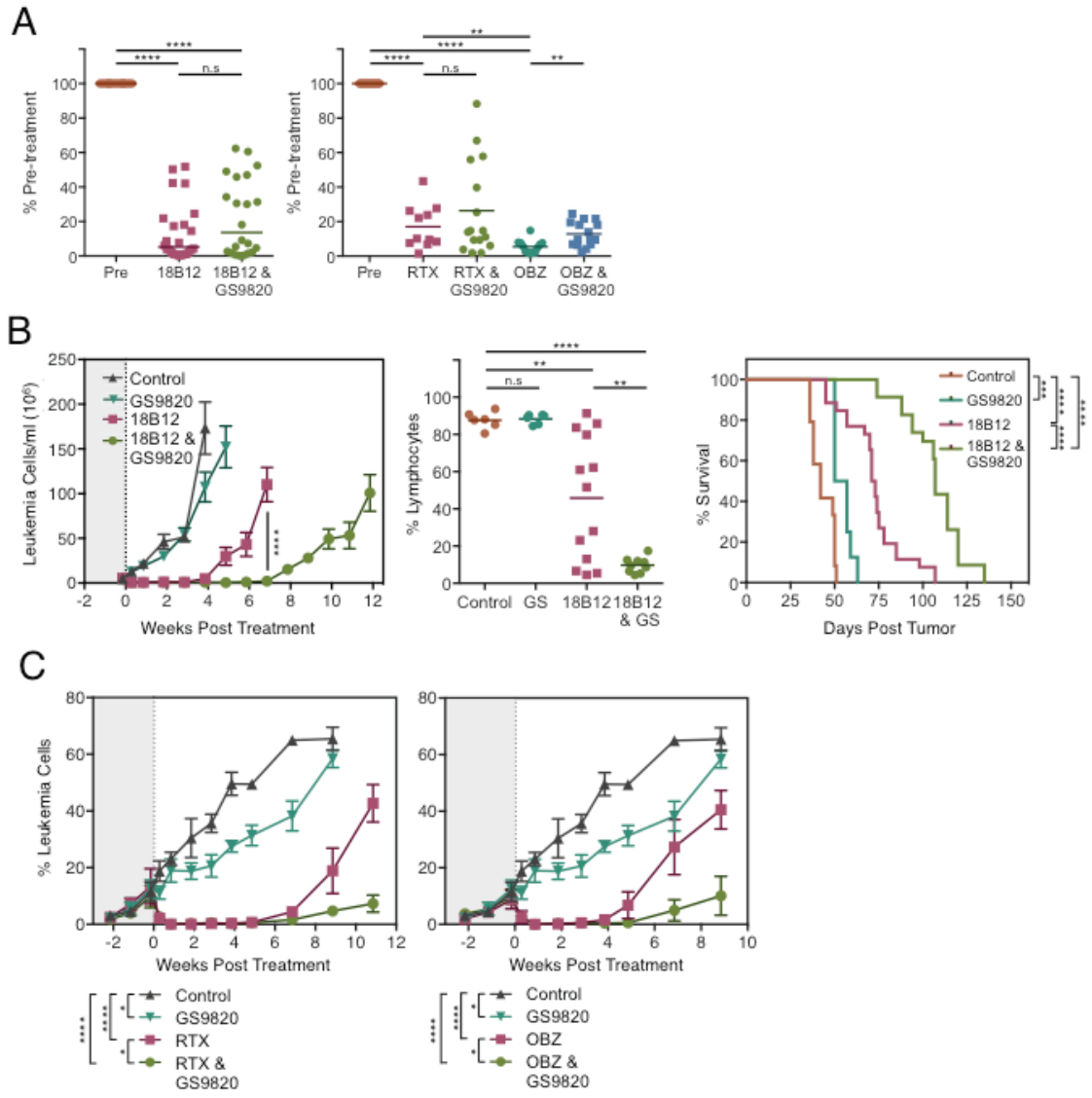


596

**Supplementary Figure.** Tumor tissue deposits and the relative efficacy of rituximab and obinutuzumab. **(A)** Animals bearing an alternate Eμ-TCL1 Tg leukemia (Eμ-TCL1 Tg U3) were treated with 250 μg anti-mouse CD20 alongside 10 mg/kg GS-9820 administered per o.s. BID or an appropriate vehicle control and monitored for peripheral leukemia levels by blood sampling and flow cytometry (shown left). Splenomegaly was assessed by palpation 3 weeks post

treatment and scored by an arbitrary system, in which a non-tumor bearing C57BL/6 is scored as 0 and a tumour bearing spleen 1 inch in length scored as 3. GS denotes GS9820. **(B)** Animals bearing different hCD20Tg Eμ-TCL1 Tg tumors (either FU2 or EC2) were assessed for the relative efficacy of rituximab (RTX) or obinutuzumab (OBZ) therapy (both hIgG1). Animals were treated with 250 μg RTX or OBZ once leukemias were detectable in the blood and monitored for disease progression by blood sampling and flow cytometry. Error bars represent SEM. Statistical analysis was performed using an un-paired Student's T test. * = p< 0.05, ** = p< 0.005, *** = p< 0.0005, **** = p< 0.00005.